Stabilization of Stochastic Linear Continuous-Time Systems using Noisy Neuromorphic Vision Sensors

Prince Singh [a,⋆] Sze Zheng Yong [b,⋆] Emilio Frazzoli [c]

***Abstract*— Vision-based robotic applications with aggressive maneuvers suffer from the low sensing speed of standard cameras that sample frames at constant time intervals. On the other hand, although neuromorphic vision sensors are promising candidates to provide the needed high-frequency sensing, a new class of algorithms needs to be synthesized that can deal with the uncommon output from each pixel of these sensors, which (independently of other pixels) fire an asynchronous stream of "retinal events" once a change in the light field is detected. In this paper, we investigate the problem of stabilizing a stochastic continuous-time linear time invariant system using noisy measurements from a neuromorphic vision sensor. We propose an H_∞ controller that addresses this problem and provide the critical event-generation threshold for these neuromorphic vision sensors and characterize the statistical properties of the resulting states. The efficacy of our approach is illustrated on an unstable system.**

I. Introduction

Regular cameras (e.g., CCD-, CMOS-based) are extensively used for many robotic and vision based applications. However, the usage of these cameras for high speed robotic applications are limited, in particular, due to their: 1) low temporal discretization (i.e., lack of information between consecutive frames), 2) redundant data (i.e., the frames contain the same information of the scene even though there was no change in the scene's brightness content), and 3) huge lag between capturing and processing (e.g., extracting features) each frame. All of these demerits hint towards a need to consider other classes of vision sensors.

In this work we consider a bio-inspired event-based (neuromorphic) vision sensor whose development has been geared towards capturing the sophistication of the photosensitive cells in the retina of living organisms that respond to changes in illumination. Each pixel of a neuromorphic vision sensor operates independently of other pixels and fires an asynchoronous (rather than fixed interval frames output by regular cameras) stream of brightness changes (i.e., "retinal events") in the order of microseconds at the time they occur. These events are generated once the observed light field changes by more than a user-chosen threshold [1]. The Dynamic Vision Sensor (DVS) is the first commercially available neuromorphic vision sensor [2].

The DVS addresses the demerits 1)-3) of conventional cameras outlined in the first paragraph. For instance, the retinal events are information bearing and so one avoids processing redundant data as with camera frames. The DVS has additional nice properties, e.g., micro-second temporal resolution, low-latency (order of micro-seconds) resulting in increased reactivity, high dynamic range ($> 120dB$) and low power requirement, collectively making it a viable sensor for enabling the quick computation of control commands to facilitate aggressive maneuvers of agile robots.

Literature Review. Most existing vision based control approaches of mobile robots rely on algorithms that are specifically developed to process the frames from regular cameras. In view of the DVS' interesting properties, a handful of recent works have been dedicated to apply these neuromorphic vision sensors to a range of specific tasks, e.g., for stabilizing the upright position of robotic insects [3], for balancing an inverted pencil [4] and for controlling an autonomous goalie [5]. Its use has also been suggested for enabling high speed collision-free flights of autonomous micro-aerial vehicles in complex environments [6].

While each pixel of an DVS should *ideally* fire a retinal event once a change in the brightness has been detected, this is not generally the case. In practice, a considerable number of false events are produced (cf., e.g., [7]) and we shall term these false events as "spurious events". There were several attempts in [7], [8] to model the generation of spurious events through suitable noise processes. The work in [7] modeled these as independent Poisson processes and proposed a proportional-derivative control scheme based on the DVS' spurious measurements with this model for the task of heading regulation. For a similar task, the author of [8] modeled ambiguities in the generation of the retinal events through a diffusion process, deriving its inspiration from noise models that have been used to study the event activity in biological neurons, e.g., see [9], [10]. These works modeled the event activity of neurons through an Ornstein-Uhlenbeck process [11]. This Gauss-Markov process captures the diffusion that triggers a neuronal spike at the crossing of a threshold and resets the process once an event is produced, a model for spurious events that we will also adopt in this paper.

⋆ Equal contribution from these authors.

[a] P. Singh is with the Laboratory for Information and Decision Systems, Massachusetts Institute of Technology, Cambridge, MA, USA (e-mail: prince1@mit.edu).

[b] S.Z Yong is with the School for Engineering of Matter, Transport and Energy, Arizona State University, Tempe, AZ, USA (e-mail: sze.zheng.yong@asu.edu).

[c] E. Frazzoli is with the Institute for Dynamic Systems and Control, Swiss Federal Institute of Technology (ETH), CH-8092 Zürich, Switzerland (e-mail: efrazzoli@ethz.ch).

This work was done at the Laboratory for Information and Decision Systems at Massachusetts Institute of Technology (MIT) and was supported by the Singapore National Research Foundation through the SMART Future Urban Mobility project.

Moreover, the proposed control approaches in all the above works with the DVS are problem-specific and share a common theme of first computing explicit state estimates and then using these estimates for closed-loop control. But, less restrictive conditions may be achieved by designs that directly use the events for control rather than performing control via state-estimation. Moreover, existing event-based control techniques, e.g., [12] are not readily applicable. Instead of having the flexibility to design a sensor (hence, events) to guarantee some performance requirement, we are given a sensor and are restrained by its inherent properties (i.e., with no means of controlling the retinal events except threshold design).

Contributions. To our best knowledge, this paper is the first to address the control of a stochastic continuous-time linear time invariant (LTI), multiple input single output (MISO) system directly from asynchronous and spurious neuromorphic measurements/events arriving from a DVS without explicit state estimation. This work builds on the authors' past work [13] where the *quadratic stabilization* of a deterministic plant with deterministically generated retinal events was considered. Intuitively, the continuity of the ambiguous neuromorphic measurements enables us to characterize the lowest upper bound on the relative uncertainty between the inaccessible continuous-time output and our estimate of this output using the retinal events/measurements we observe. Then, by designing an H_∞ controller that is robust to this uncertainty, we are able to stabilize the first moment of the noisy hybrid system and derive the corresponding critical event threshold required for a DVS to perform this stabilization. Moreover, we characterize the statistical properties of the system states when using our feedback controller.

Our solution makes use of some ideas and tools drawn from the literature on control with limited information, in particular, the quantized control literature, e.g., [14], [15], [16]. Additionally, the extension of the present work for the stabilization and regulation of a multiple input multiple output (MIMO) noisy system with ambiguous measurements can be readily adapted following [17].

Outline. This paper is organized as follows. In Section II, we formulate the problem by first characterizing the DVS model and the stochastic noise model, as well as represent the combined LTI system and DVS model as a noisy hybrid system. Then, in Section III, we design a stabilizing controller for this hybrid system and present a criterion that provides us with the least restrictive (largest) event threshold that is required of a DVS to stabilize the given LTI system. We also provide statistical properties of the resulting system states. In Section IV, we demonstrate the effectiveness of our approach via a numerical experiment. Finally, in Section V, we present conclusions and outline possible future work.

II. Problem Formulation

LTI System. Consider the unstable, single input, stabilizable and detectable continuous time system (see [17] for a physical example) given by,

$$\begin{aligned} \dot{x} &= Ax + Bu + w, \quad x(0) \sim \mathcal{N}(x_0, P_0), \\ \tilde{y} &= c'x, \end{aligned} \tag{1}$$

where $x(t) \in \mathbb{R}^n$ is the system's state with $A \in \mathbb{R}^{n\times n}$, $u \in \mathbb{R}^m$ is the control input to the system with $B \in \mathbb{R}^{n\times m}$, $w \sim \mathcal{N}(0, Q)$ is the process noise with $Q \succeq 0$ (positive semidefinite), and $\tilde{y} \in \mathbb{R}$ is a scalar output of the system with $c \in \mathbb{R}^{n\times 1}$. The first two moments of the initial state, x_0 and $P_0 \succeq 0$, are unknown but assumed to be bounded. Note that we have no direct access to the output $\tilde{y}$, except through the "retinal event" measurements that we obtain from a neuromorphic camera, which we characterize next.

DVS Model. Our sensor of choice is the Dynamic Vision Sensor (DVS), which is the first commercially available neuromorphic sensor [2]. An *ideal* noiseless DVS comprises of a photodiode that converts luminosity to a photocurrent, denoted by $\tilde{y}$ as in (1) that is then amplified in a logarithmic fashion to detect brightness changes in real time. However, these sensors are known to produce a considerable number of spurious events [7].

In order to account for spurious events, we draw inspiration from the event activity in biological neurons as discussed in Section I, and consider a Gauss-Markov process known as Ornstein-Uhlenbeck process [11] as our noise model:

$$\dot{v} = \left(\frac{-1}{2\tau_c}\right) v + (\sigma_v)\eta, \tag{2}$$

where the time constant $\tau_c > 0$ is of the order of micro-seconds due to the DVS' micro-second temporal resolution, and with $\eta \sim \mathcal{N}(0, 1)$ being a scalar zero-mean unit-variance Gaussian white noise that is statistically independent from w. Additionally, the mean and variance of (2) starting at $v(0)$ is easily found to be (for $t \geq 0$) (see, e.g., [11])

$$\mu(t) = v(0)e^{-\frac{t}{2\tau_c}}, \tag{3}$$

$$\sigma^2(t) = \sigma_v^2\tau_c\left(1 - e^{-\frac{t}{\tau_c}}\right), \tag{4}$$

and $\sigma_v^2\tau_c$ represents the steady-state covariance of the stationary Gauss-Markov process (2). Then, we model the spurious events through the corruption of the *trigger condition*, upon which "retinal events" are generated by each pixel of the DVS as follows:

$$|\tau| \geq h, \tag{5}$$

where

$$\tau \triangleq \log_e|\tilde{y}| + v - \log_e|q|, \tag{6}$$

and $q \in \mathbb{R}$ is the trigger reference (an internal state that resets every time an event is triggered) and $h > 0$ is a user-defined event threshold. Equivalently, we can consider the output y (that we still do not have access to) as the *ideal* output $\tilde{y}$ that is corrupted by a parametric noise e^v with a log-normal distribution as follows

$$y = \tilde{y}e^v = c'xe^v, \tag{7}$$

and thus, $\tau = \log_e |y| - \log_e |q|$. Using the terminology for a hybrid system model, the trigger condition (5) is a stochastic guard set, which we denote as $\mathcal{D}$, i.e., a "retinal event" occurs when the combined system (LTI system and DVS model) state satisfies the guard condition, $\mathbf{x} := [x^\top, q]^\top \in \mathcal{D}$.

The k-th "retinal event" is then given by the triple: $\langle t_k, \langle x_i(t_k), y_i(t_k)\rangle, p(t_k)\rangle$ where t_k denotes the timestamp at which the "retinal event" was fired, $\langle x_i(t_k), y_i(t_k)\rangle$ represent the pixel coordinates of the i'th pixel where a "retinal event" was fired and $p(t_k)$ is the polarity measurement we obtain that we will describe next. However, in this paper, we will only discuss the single pixel case, hence we have a scalar output y. The extension to the case of multiple outputs is straightforward and can be done following [17].

As we previously described, we have no access to this output y (nor $\tilde{y}$), but instead we have access to polarity measurements, $p \in \{-1, 0, +1\}$ given by the events:

$$p = \begin{cases} \text{sgn}(\tau), & \text{if } \mathbf{x} \in \mathcal{D}, \\ 0, & \text{otherwise.} \end{cases} \tag{8}$$

Due to the continuity of the output trajectory y, which is characterized by the continuous solution of (2), we know that the event trigger for the DVS always takes place when equality holds for the trigger condition (5). Thus, the evolution of the trigger reference is described by

$$q^+ = q\rho^{-p}, \tag{9}$$

where for convenience, we define

$$\rho \triangleq e^{-h} \in (0, 1), \tag{10}$$

as the spacing of the logarithmic partitions induced onto the output space by the logarithmic *trigger condition* in (5). This choice of ρ in (10) captures the range of positive values for the event threshold h of the DVS. Then, the *trigger condition* (5) can be equivalently re-written as

$$\mathcal{D} \triangleq \{\mathbf{x} : \left|\frac{y}{q}\right| \geq \frac{1}{\rho} \text{ or } \left|\frac{y}{q}\right| \leq \rho\}, \tag{11}$$

which explicitly defines our guard set $\mathcal{D}$ in terms of ρ.

Further, we make the following assumption regarding the trigger reference q:

(A1) The initial trigger reference $q(0)$ lies in the interval: $m \leq q(0) \leq M$ where $0 < m \leq M$ are scalars and satisfies $\rho < \left|\frac{y(0)}{q(0)}\right| < \frac{1}{\rho}$ with $y(0) \in \mathcal{D}^c$, the complement of the guard set $\mathcal{D}$.

(A2) The sign of q is known at all times.

The first assumption is more realistic than the assumption made in our previous work [13] in that the luminosity of the environment that a DVS is turned on in may not be known exactly, but is only known to be within some bound. Intuitively, this assumption along with the continuity of the output trajectory makes it possible to keep track of the internal trigger reference at all times. The latter assumption is only necessary for theoretical analysis when considering the general LTI system. In practice, the luminosity is always positive, hence q is also always positive.

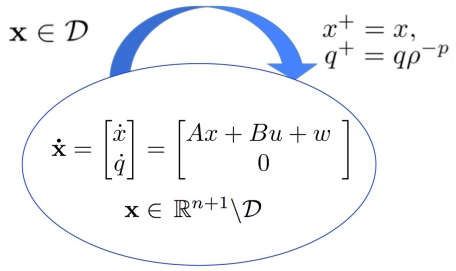

Fig. 1: Open loop hybrid automaton of combined LTI system and DVS model in (12), where p and $\mathcal{D}$ are given in (8) and (11), respectively.

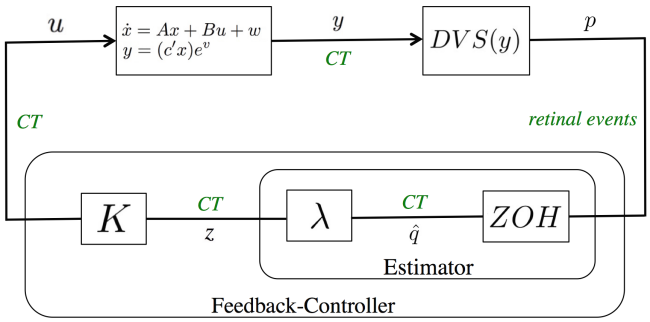

Fig. 2: Controller design approach: From asynchronous retinal events to continuous-time (CT) control commands.

Combined System. Combining the LTI system in (1) and DVS model in (9) yields the following noisy hybrid system:

$$\begin{aligned} \dot{\mathbf{x}} &= \begin{bmatrix} \dot{x} \\ \dot{q} \end{bmatrix} = \begin{bmatrix} Ax + Bu + w \\ 0 \end{bmatrix}, & \mathbf{x} &\in \mathbb{R}^{n+1} \backslash \mathcal{D}, \\ \dot{\mathbf{x}}^+ &= \begin{bmatrix} x^+ \\ q^+ \end{bmatrix} = \begin{bmatrix} x \\ q\rho^{-p} \end{bmatrix}, & \mathbf{x} &\in \mathcal{D}, \end{aligned} \tag{12}$$

where the polarity measurement p is given in (8) and the stochastic guard set $\mathcal{D}$ in (11). The hybrid automaton that results is illustrated in Figure 1.

Thus, the stabilizing control problem with the DVS is:

Problem 1. *The* objective *of this paper is two-fold:*

1) *Design a feedback controller u using the polarity measurement p from a DVS, as in* (8)*, to stabilize the first moment of the noisy hybrid system given in* (12)*, i.e.,* $\lim_{t\to\infty} \mathbb{E}[x(t)] = 0$*. Moreover, quantify the least restrictive (largest) upper-bound on the event threshold h^*, such that for any DVS with event threshold $h < h^*$, the controller u meets the aforementioned objective.*
2) *For the stabilizing controller designed for Problem 1-1, characterize the statistical properties of the resulting system states $x(t)$.*

III. Controller Design

In this section, we will first design a feedback controller that operates on the incoming polarity measurements p (i.e., based on the "noisy" *trigger condition* in (5)) to generate a continuous time control signal u that solves Problem 1-1, i.e., one that stabilizes the first moment of the noisy LTI system (12). We are inspired by output feedback control, thus we construct an estimator for the output signal y in Section III-A

and use the resulting estimate z as an input to our controller K, which we will design in Section III-B. This cascade set-up of the feedback controller, which consists of the estimator and the feedback controller is depicted in Figure 2. In turn, we will derive the statistical properties of the true system states, i.e., solve Problem 1-2.

A. Design of estimator for y

Since we know that event trigger for the DVS always takes place when equality holds for the trigger condition (5) and the output trajectory y is continuous (cf. (2)), q coincides with y whenever an event is produced. Hence, as depicted in Figure 2, it seems natural to consider a scaled estimate of q as an estimate of y

$$z \quad = \lambda \hat{q}, \quad 0 \neq \lambda \in \mathbb{R}, \tag{13}$$

where λ is the scaling and $\hat{q}$ is an estimate of q, which we will derive next.

As there is no additional sensor to appropriately quantify the lack of information between the retinal events, we consider a Zero-Order-Hold (ZOH) on the retinal events arriving from the DVS and an estimate of the trigger reference q that follows the same evolution of (9) (cf. [17] for an illustration of the its evolution):

$$\hat{q}^+ = \hat{q}\rho^{-p}, \tag{14}$$

where $\hat{q}(0)$ and $\hat{q}(t)$ are characterized in the following.

Lemma 1. *[17, Lemmas 1 and 2] The evolution of the estimate of the trigger reference $\hat{q}(t)$ for all t,*

$$\hat{q}(t) = (1 + \Delta_q)q(t), \ |\Delta_q| \leq \delta_q, \tag{15}$$

yields the least restrictive z in (13)*, if $\hat{q}(0)$ is chosen as*

$$\hat{q}(0) = \frac{2mM}{M+m},$$

which produces the minimal $|\Delta_q|$ with bounds,

$$\delta_q = \frac{M-m}{M+m}.$$

Moreover, we can quantify the closeness of the designed continuous-time signal z to the unknown output y, given in the following lemma and visualized in Figure 3.

Lemma 2. *[17, Lemma 3] The estimate $\hat{q}$ estimates y with bounded (asymmetric) uncertainty:*

$$\rho y \leq q = \frac{\hat{q}}{1+\Delta_q} \leq \frac{y}{\rho}. \tag{16}$$

Note that Figure 3 was given with unit amplification, $\lambda = 1$, i.e., $z = \hat{q}$, which illustrates the unequal length of the line segments representing positive ($p = +1$) and negative ($p = -1$) transitions in blue and red, respectively. Intuitively, these unequal lengths motivate the need for the scaling λ which provides us a symmetric bound on the absolute relative error between z and y signals.

Lemma 3. *The absolute relative error between the*

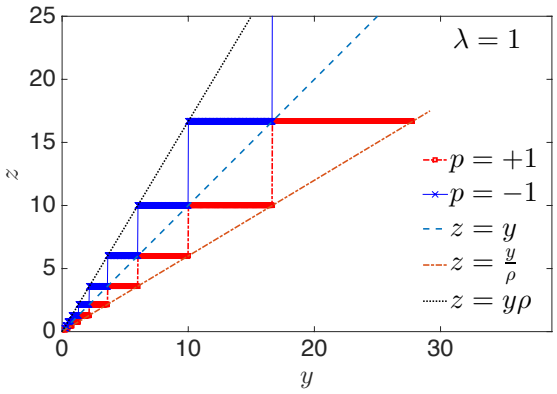

Fig. 3: Analysis of the signal z ($\lambda = 1$): Red/solid lines are due to positive transitions ($p = +1$) while blue/solid-star lines are due to negative transitions ($p = -1$).

1) *z and y signals is upper-bounded,*

$$|\Delta_z| \leq \delta_z,$$

where $\Delta_z \triangleq \frac{z-y}{y}$, $z = \lambda\hat{q}$ and y given in (7)*,*

2) *$\bar{z} \triangleq \mathbb{E}[z]$ and $\bar{y} \triangleq \mathbb{E}[y]$ signals is also upper-bounded*

$$|\bar{\Delta}_z| \leq \delta_z,$$

where $\bar{\Delta}_z \triangleq \frac{\bar{z}-\bar{y}}{\bar{y}}$,

with a symmetric upper-bound $\delta_z \triangleq \frac{M-m\rho^2}{M+m\rho^2}$ when we choose $\lambda \triangleq \frac{(M+m)\rho}{M+m\rho^2}$.

Proof. See Lemma 4 of [17] for the proof of 1). To see 2), note that the final inequality in the proof of Lemma 4 in [17] is given by

$$(1-\delta_z)y \leq z - y \leq (1+\delta_z)y.$$

Then, taking the expectation of the previous inequality gives,

$$-\delta_z \leq \frac{\bar{z}-\bar{y}}{\bar{y}} \leq \delta_z,$$

thus, the result follows. ■

In fact, our choice of $\hat{q}(0)$ and λ, that results in symmetric upper-bounds is *optimal*, formally stated below.

Proposition 1. *[17, Theorem 3] The choice of $\hat{q}(0)$ and λ in Lemmas 1 and 3 leads to the least restrictive (smallest) ρ, which will lead to the least restrictive threshold h (cf.* (10)*).*

B. Design of feedback controller K

To solve Problem 1-1, instead of directly synthesizing a stabilizing controller for the uncertain noisy hybrid system of (12), which may be difficult and even harder to analyze, we resort to finding sufficient conditions for stabilizing the first moment of this noisy hybrid system by considering the stability of a deterministic auxiliary uncertain system in the following proposition, and analyze the resulting statistical properties of the system states later.

Proposition 2. *The first moment of the noisy hybrid system* (12)*—with (A, B, c') stabilizable, detectable and $\rho \in (0, 1)$ —can be stabilized via the linear controller K through the*

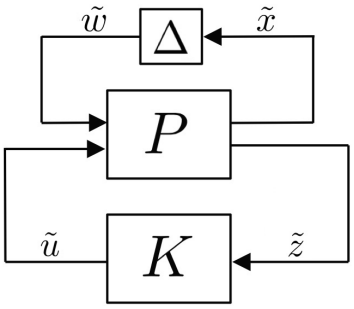

Fig. 4: H_∞ control problem with generalized plant P and controller K given in (19) and (20), respectively.

control law $u = K\frac{z}{\mathbb{E}[e^v]}$ *with* $\mathbb{E}[e^v] = e^{\left(\mu+\frac{\sigma^2}{2}\right)}$ *whose parameters are defined in* (3) *and* (4)*, respectively, if the following deterministic auxiliary uncertain system*

$$\begin{aligned} \dot{\tilde{x}} &= A\tilde{x} + B\tilde{u}, \\ \tilde{z} &= (1+\Delta)c'\tilde{x}, |\Delta| \leq \delta_z \end{aligned} \tag{17}$$

can be quadratically-stabilized via the controller K*, with* $\tilde{u} = K\tilde{z}$ *and* δ_z *given in Lemma 3.*

Proof. First, taking the expectation of $u = K\frac{z}{\mathbb{E}[e^v]}$, we have

$$\begin{aligned} \bar{u} \triangleq \mathbb{E}[u] = K\frac{\mathbb{E}[z]}{\mathbb{E}[e^v]} &= K(1+\bar{\Delta}_z)\frac{\bar{y}}{\mathbb{E}[e^v]}, \\ &= K(1+\bar{\Delta}_z)c'\bar{x}, \end{aligned}$$

where $\mathbb{E}[z] \triangleq \bar{z} = (1+\bar{\Delta}_z)\bar{y}$ in view of the second result of Lemma 3, and taking the expectation of (7) with e^v being independent of x and $\bar{x} \triangleq \mathbb{E}[x]$ is the first moment of the system state. Moreover, taking the expectation of the state equation in (1) and substituting $\bar{u}$, we obtain

$$\begin{aligned} \dot{\bar{x}} &= A\bar{x} + B\bar{u} \\ &= A\bar{x} + BK(1+\bar{\Delta}_z)c'\bar{x}. \end{aligned}$$

This is clearly an instance of (17) with $\bar{x} \equiv \tilde{x}$, $\bar{u} \equiv \tilde{u} = K\tilde{z}$ and $\bar{\Delta}_z \equiv \Delta$. Thus, the proposition holds directly.

Furthermore, $\mathbb{E}[e^v] = e^{\left(\mu+\frac{\sigma^2}{2}\right)}$ can be computed from the properties of a log-normal distribution. ■

We are now ready to state the solution to Problem 1-1 in the following theorem.

Theorem 1. *The first moment of the noisy hybrid system* (12)*—with* (A, B, c') *stabilizable, detectable and* $\rho \in (0,1)$ *—can be stabilized via an* H_∞ *controller, provided that the event threshold* h *in* (5) *of the DVS is upper-bounded by*

$$h < h^\star = \log_e \sqrt{\left(\tfrac{m}{M}\right)\tfrac{\gamma+1}{\gamma-1}}, \tag{18}$$

where $\gamma > 1$ *is the* H_∞ *norm of the closed-loop uncertain system* (17)*.*

Proof. This result is an adaptation of Theorem 2 of [17]. However, for completeness we briefly re-state here the essential parts of the proof.

Due to the presence of a bounded uncertainty Δ in the deterministic auxiliary uncertain system (17), it is natural to represent the problem in the Robust Control framework. The

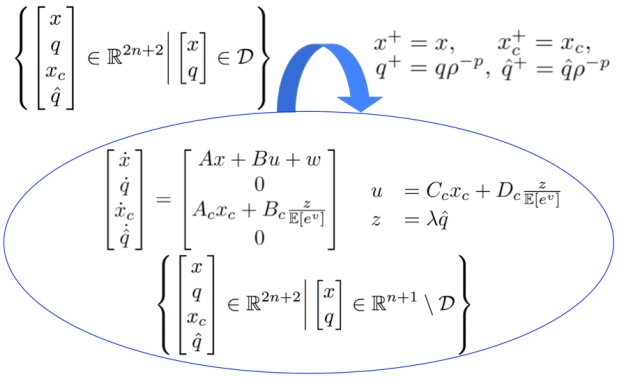

Fig. 5: Closed loop hybrid automaton of combined LTI system, DVS model and H_∞ controller, where τ and $\mathcal{D}$ are given in (6) and (11), respectively, and with $h < h^*$ in Theorem 1 and $\mathbb{E}[e^v] = e^{\left(\mu+\frac{\sigma^2}{2}\right)}$.

H_∞ control problem that results for this closed loop system is shown in Figure 4 with the generalized plant P

$$P = \left[\begin{array}{c|cc} A & 0_{n\times n} & B \\ \hline I_{n\times n} & 0_{n\times n} & 0_{n\times m} \\ c' & c' & 0_{1\times m} \end{array}\right] \tag{19}$$

and the state space description of the H_∞ controller K

$$K = \left[\begin{array}{c|c} A_c & B_c \\ \hline C_c & D_c \end{array}\right], \tag{20}$$

with input $\tilde{z}$ and can be synthesized under some mild assumptions given in [18].

Then, the finite H_∞ norm of the closed-loop system (P, K) in Figure 4 is found as $||T_{\tilde{x}\tilde{w}}(s)||_{H_\infty} < \gamma$, via a γ-iteration algorithm [18], where $T_{\tilde{x}\tilde{w}}(s)$ is the transfer function from the bounded disturbance $\tilde{w}$ due to Δ to the performance variable $\tilde{x}$.

Finally, the application of the small gain theorem yields the upper bound on δ_z, such that $|\Delta| \leq \delta_z$,

$$\delta_z < \delta_z^* \triangleq \frac{1}{\gamma},$$

which can be tolerated to render the closed loop system (P, K, Δ) quadratically stable or equivalently robustly asymptotically stable [19].

Now, in view of $\delta_z = \frac{M-m\rho^2}{M+m\rho^2}$ from Lemma 3, we obtain $\rho^* = \sqrt{\left(\frac{M}{m}\right)\frac{\gamma-1}{\gamma+1}}$. Next, from our definition of ρ in (10), we obtain an upper bound on the tolerable event threshold

$$h < h^\star \triangleq \log_e \sqrt{\left(\frac{m}{M}\right)\frac{\gamma+1}{\gamma-1}}.$$

Finally, by Proposition 1, the H_∞ controller also stabilizes the first moment of the noisy hybrid system (12). ■

In summary, the resulting closed loop hybrid automaton that combines the different steps in the design of K, λ and $\hat{q}$ is illustrated in Figure 5.

C. Statistical properties of system states x

We now investigate the properties of the system states x and state the solution to Problem 1-2 in the following.

Theorem 2. *For the controller K designed in Theorem 1, the closed-loop noisy hybrid system (12) has a solution $\{x(t)\}$ on the time-interval $[0,T]$ in the mean square sense. Moreover, this solution has these additional properties:*

1) *The first moment of the system is quadratically stable; so, $\lim_{t\to\infty}\mathbb{E}[x(t)]=0$.*
2) *$\{x(t)\}$ is mean square continuous in $[0,T]$.*
3) *The trace of the second moment of the system—$P_t \triangleq \mathbb{E}[x(t)x(t)^T]$—is finite, i.e., $\mathrm{trace}(P_t) = \mathbb{E}[x(t)^T x(t)] = \mathbb{E}[\|x(t)\|^2] < \infty$ is finite $\forall t \in [0,T]$.*
4) *$\int_0^T \mathbb{E}[\|x(t)\|^2]dt < \infty$.*
5) *$x(t)-x_0$ is independent of $\{dw(\tau), \tau \geq t\}$ for every $t \in [0,T]$.*

Additionally, the process $\{x(t)\}$ is a Markov process and, in the mean square sense, is uniquely determined by the initial condition x_0.

Proof. The proof of 1) follows from Theorem 1. To show that the rest of the properties holds, we note that the continuous dynamics of our closed loop stochastic differential equation (SDE) is readily found upon combining the LTI system in (1) with the control law $u = K\frac{z}{\mathbb{E}[e^v]}$ where K is given in (20) to obtain

$$d\begin{bmatrix}x\\x_c\end{bmatrix} = \left(\begin{bmatrix}A & BC_c\\0 & A_c\end{bmatrix}\begin{bmatrix}x\\x_c\end{bmatrix} + \begin{bmatrix}BD_c\\B_c\end{bmatrix}\frac{z}{\mathbb{E}[e^v]}\right)dt + \begin{bmatrix}I\\0\end{bmatrix}dw$$

with $\mathbb{E}[e^v] = e^{\left(\mu+\frac{\sigma^2}{2}\right)}$. The signal z, given in (13) and (14), remains constant between events, thus the continuous dynamics above is a linear SDE between events. Moreover, during the 'retinal' events, the continuous states do not jump, i.e., $x^+ = x$ and $x_c^+ = x_c$. Hence, in the parlance of hybrid systems, we have a stochastic switched linear system.

During continuous flow (between events), since we have a linear SDE, it can be easily verified that the assumptions in [20, Theorem 4.5] are satisfied and hence, all the other properties (besides 1) hold during continuous flow. On the other hand, during the events, the continuous closed loop states do not jump and thus, the statistical properties of the states, which include x, are not affected in the mean square sense (cf. relevant definitions, e.g., mean square continuity, in [20]). Therefore, the theorem holds. ■

IV. Numerical Experiment

We now demonstrate the effectiveness of our proposed approach with the following unstable, but stabilizable and detectable, system:

$$A = \begin{bmatrix}2 & 10\\0 & 5\end{bmatrix},\quad B = \begin{bmatrix}1\\1\end{bmatrix},\quad c = \frac{1}{\sqrt{5}}\begin{bmatrix}2\\1\end{bmatrix},$$

with $Q = 0.03\cdot I_{2\times 2}$. First, we design an H_∞ controller for the auxiliary uncertain system in (17) through the `hinfric` command in MATLAB, with $m = M = 1$ in assumption (A1), $\tau_c = 10^{-3}$ (sec) and $\sigma_v = 50$ in (2) and obtain

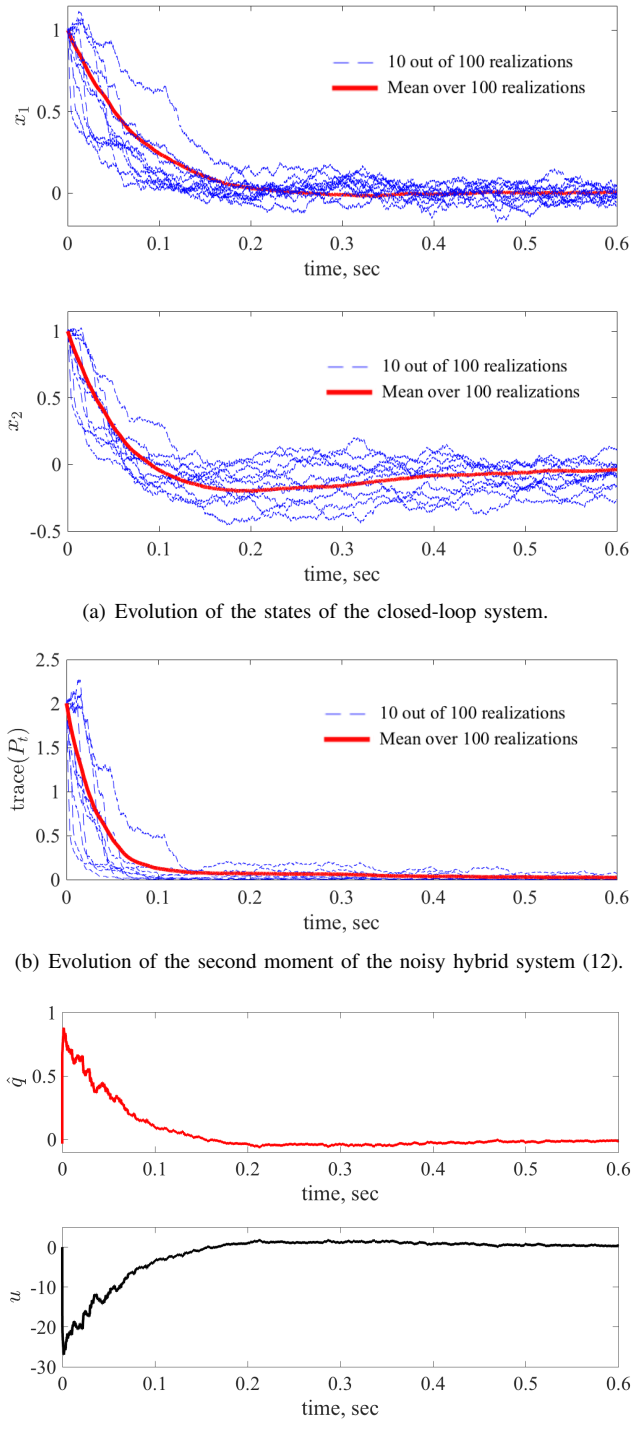

(a) Evolution of the states of the closed-loop system.

(b) Evolution of the second moment of the noisy hybrid system (12).

(c) Estimate of the trigger reference and the control command for an example realization.

Fig. 6: Numerical Example: Stabilization of a stochastic unstable system.

$\gamma = 1.3867$ and $h^* = 0.9100$. Then, we utilize this H_∞ controller for the true system (1). The noisy hybrid system (12) was discretized and integrated via the Euler-Maruyama scheme with a temporal discretization of 10^{-6} (sec). The simulation results are presented in Figure 6. Figure 6(a) shows that the controller stabilizes the first moment of the system. It can be observed that the realizations of the plant

become concentrated near the origin with increasing time. On the other hand, Figure 6(b) also shows that the trace of the second moment, $\mathrm{trace}(P_t) \triangleq \mathbb{E}[x^T x] = \mathbb{E}[x_1^2 + x_2^2]$, remains finite and appears to converge to a finite value. For completeness, we also plotted the estimate of the trigger reference and the corresponding command inputs for a representative realization in Figure 6(c).

V. Conclusions and Future Work

The Dynamic Vision Sensor (DVS) is a neuromorphic sensor, which is a recent addition to the class of vision sensors. The nice properties of the DVS promise to facilitate agile robotic maneuvers. However, existing vision algorithms cannot be directly adapted to process these events; thus, new algorithms need to be developed.

In this work, we proposed an H_∞ controller that stabilizes the first moment of noisy unstable LTI systems using DVS' noisy measurements, while showing that the resulting system states have nice statistical properties. In addition, we also provide the least restrictive upper bound on the event threshold, h^*, for the DVS such that the pair (A, B) is stabilized. This work can be viewed as an initial attempt to locally stabilize a noisy nonlinear system about some operating point using corrupted DVS measurements.

There are many interesting directions for future research. An important one is to develop a control scheme that can handle an accurate description of the environment's luminance, e.g., through an integrative sensor model, since a linear varying luminance profile may not be regularly encountered in practice. Finally, it would be crucial to develop control schemes for multiple input multiple output (MIMO) systems that have a nonlinear description, e.g., by first considering linear time-variant systems [21], to tackle real world applications. The issue of designing stabilizing controllers for systems with a nonlinear description has been acknowledged by related works as being the bottleneck to facilitate basic control-theoretic applications with neuromorphic sensors. The robust framework of the current work may serve as a viable route to tackle this problem.

References

[1] Shih-Chii Liu and Tobi Delbruck. Neuromorphic sensory systems. *Current opinion in neurobiology*, 20(3):288–295, 2010.

[2] Patrick Lichtsteiner, Christoph Posch, and Tobi Delbruck. A 128×128 120 db 15 μs latency asynchronous temporal contrast vision sensor. *Solid-State Circuits, IEEE Journal of*, 43(2):566–576, 2008.

[3] Sawyer B Fuller, Michael Karpelson, Andrea Censi, Kevin Y Ma, and Robert J Wood. Controlling free flight of a robotic fly using an onboard vision sensor inspired by insect ocelli. *Journal of The Royal Society Interface*, 11(97):20140281, 2014.

[4] Jörg Conradt, Matthew Cook, Raphael Berner, Patrick Lichtsteiner, Rodney J Douglas, and T Delbruck. A pencil balancing robot using a pair of aer dynamic vision sensors. In *Circuits and Systems, 2009. ISCAS 2009. IEEE International Symposium on*, pages 781–784. IEEE, 2009.

[5] Tobi Delbruck and Manuel Lang. Robotic goalie with 3 ms reaction time at 4% cpu load using event-based dynamic vision sensor. *Neuromorphic Engineering Systems and Applications*, page 16, 2015.

[6] Andrew J Barry and Russ Tedrake. Pushbroom stereo for high-speed navigation in cluttered environments. In *Robotics and Automation (ICRA), 2015 IEEE International Conference on*, pages 3046–3052. IEEE, 2015.

[7] Erich Mueller. *Feedback Control of Dynamic Systems with Neuromorphic Vision Sensors*. PhD thesis, Massachusetts Institute Of Technology, October 2015.

[8] Andrea Censi. Efficient neuromorphic optomotor heading regulation. In *American Control Conference (ACC), 2015*, pages 3854–3861. IEEE, 2015.

[9] Frederic YM Wan and Henry C Tuckwell. Neuronal firing and input variability. *J. theor. Neurobiol*, 1(2):197–218, 1982.

[10] RM Capocelli and LM Ricciardi. Diffusion approximation and first passage time problem for a model neuron. *Kybernetik*, 8(6):214–223, 1971.

[11] George E Uhlenbeck and Leonard S Ornstein. On the theory of the brownian motion. *Physical review*, 36(5):823, 1930.

[12] Karl J Aström. Event based control. In *Analysis and design of nonlinear control systems*, pages 127–147. Springer, 2008.

[13] Prince Singh, Sze Zheng Yong, Jean Gregoire, Andrea Censi, and Emilio Frazzoli. Stabilization of linear continuous-time systems using neuromorphic vision sensors. In *IEEE Conference on Decision and Control*. IEEE, 2016.

[14] Nicola Elia and Sanjoy K Mitter. Stabilization of linear systems with limited information. *Automatic Control, IEEE Transactions on*, 46(9):1384–1400, 2001.

[15] Minyue Fu and Lihua Xie. The sector bound approach to quantized feedback control. *Automatic Control, IEEE Transactions on*, 50(11):1698–1711, 2005.

[16] Linh Vu and Daniel Liberzon. Stabilizing uncertain systems with dynamic quantization. In *Decision and Control, 2008. CDC 2008. 47th IEEE Conference on*, pages 4681–4686. IEEE, 2008.

[17] Prince Singh, Sze Zheng Yong, and Emilio Frazzoli. Set-point regulation of linear continuous-time systems using neuromorphic vision sensors. In *Automatic Control, IEEE Transactions on*, 2017. Submitted. Available from: `http://arxiv.org/abs/1609.05483`.

[18] John C Doyle, Keith Glover, Pramod P Khargonekar, and Bruce A Francis. State-space solutions to standard H_2 and H_∞ control problems. *Automatic Control, IEEE Transactions on*, 34(8):831–847, 1989.

[19] Andy Packard and John Doyle. Quadratic stability with real and complex perturbations. *Automatic Control, IEEE Transactions on*, 35(2):198–201, 1990.

[20] Andrew H Jazwinski. Stochastic process and filtering theory, academic press. *A subsidiary of Harcourt Brace Jovanovich Publishers*, 1970.

[21] Rajamani Ravi, Krishan M Nagpal, and Pramod P Khargonekar. H^∞ control of linear time-varying systems: A state-space approach. *SIAM Journal on Control and Optimization*, 29(6):1394–1413, 1991.